

MAJOR PAPER

Direct Impact of Motor Cortical Stimulation on the Blood Oxygen-level Dependent Response in Rats

Zonghao Xin¹, Yoshifumi Abe², Shuang Liu¹, Kenji F. Tanaka²,
Koichi Hosomi³, Youichi Saitoh³, and Masaki Sekino^{1*}

Purpose: Neuropathic pain is a complex and distressing chronic illness in modern medicine. Since 1990s, motor cortex stimulation (MCS) has emerged as a potential treatment for chronic neuropathic pain; however, the precise mechanisms underlying analgesia induced by MCS are not completely understood. The purpose of the present study was to investigate the blood oxygen-level dependent (BOLD) response in the brain during MCS.

Methods: We inserted a bipolar tungsten electrode into the primary motor cortex (M1) of adult male Wistar rats. Functional magnetic resonance imaging (fMRI) scans were implemented simultaneously with the electrical stimulation of M1 and the BOLD signals taken from the fMRI were used as an index to reflect the response against MCS.

Results: Our results demonstrated that the bilateral M1, ipsilateral caudate-putamen, and ipsilateral primary somatosensory cortex to the stimulation spot were activated after the onset of MCS. The BOLD signal time courses were analysed in these regions and similar temporal characteristics were found.

Conclusion: By conducting direct cortical stimulation of the rodent brain to investigate its instant effect using fMRI, we identified encephalic regions directly involved in the instant motor cortical stimulation effects in healthy rat models. This result may be essential in establishing a foundation for further research on the underlying neuropathways associated with the MCS effects.

Keywords: *functional magnetic resonance imaging, motor cortex stimulation, primary motor cortex, caudate-putamen*

Introduction

Neuropathic pain (NP), often caused by lesions or dysfunction in the nervous system, has become a complicated and severe syndrome in modern medicine. Patients who suffer from NP typically share the characteristic of spontaneous and ongoing pain accompanied with hyperalgesia.¹ Due to the drug resistant nature of NP, treatment for patients with chronic pain is considered to be a challenge in clinical practice.

Over the past few decades, however, motor cortex stimulation (MCS) has emerged as a potentially effective therapeutic method to control pain in patients suffering from NP.² Both mature non-invasive and invasive approaches based on MCS have been increasingly applied in the treatment of NP. Repetitive transcranial magnetic stimulation (rTMS) has been widely known as a non-invasive method to relieve NP, where alternating magnetic fields are used to generate currents in the tissue with high focality.³ Conversely, epidural and subdural MCS are representative invasive approaches where an electrode is implanted directly into the epidural or subdural motor cortex region to convey electrical current.^{4,5} However, both two types of methods share the same mechanisms of conducting electrical stimulation for pain relief.

To date, systematic studies of MCS have been established and numerous case reports have demonstrated that pain relief occurs progressively after the onset of MCS and could persist after the cessation of stimulation.^{6,7} However, the outcomes of MCS vary across individuals, which is a reflection of the complexity and discrepancy of pain

¹School of Engineering, The University of Tokyo, Tokyo, Japan

²Department of Neuropsychiatry, Keio University School of Medicine, Tokyo, Japan

³Department of Neuromodulation and Neurosurgery, Osaka University Graduate School of Medicine, Suita, Osaka, Japan

*Corresponding author: Department of Electrical Engineering and Information Systems, Graduate School of Engineering, The University of Tokyo, 7-3-1, Hongo, Bunkyo-ku, Tokyo 113-0033, Japan. Phone: +81-3-5841-7490, Fax: +81-3-5841-6688, E-mail: sekino@bee.t.u-tokyo.ac.jp

©2020 Japanese Society for Magnetic Resonance in Medicine

This work is licensed under a Creative Commons Attribution-NonCommercial-NoDerivatives International License.

Received: November 1, 2019 | Accepted: March 17, 2020

conditions, and most significantly, the lack of understanding of the mechanisms underlying MCS-induced analgesia.⁸

In the present study, we performed experiments using rat models to further investigate encephalic regions that are possibly involved in the neural activity activated by MCS using functional magnetic resonance imaging (fMRI). To investigate the immediate effects of MCS, changes in regional blood oxygen-level dependent (BOLD) signals were used as indices for assessing the fMRI data that were taken simultaneously with the stimulation.

Materials and Methods

The present study was approved by the University of Tokyo's committee on research ethics and was done in accordance with the University of Tokyo's guidelines regarding animal research (#KA12-4).

Animals

Ten adult male Wistar rats (10 weeks) weighing 280 ± 20 g were used in this study. Prior to the experiment, rats were individually reared in cages with free access to water and rat chow pellets and the room temperature was maintained at $23 \pm 2^\circ\text{C}$. Two rats were used in the preliminary experiment to test the intensity of stimulation exerted on the motor cortex as well as to obtain structural images via MRI. The remaining rats ($n = 8$) underwent craniotomy and were used in fMRI experiments to study the MCS-evoked cortical BOLD signals.

Stimulation electrode

A custom-made tungsten bipolar electrode was used to convey electrical current.⁹ Two tungsten microwires with a diameter of 50 μm and covered by polyimide insulation (California Fine Wire Co., Grover Beach, CA, USA) were straightened parallelly by hanging them between two magnetic clamps and twisting into one strand. The middle part of the electrode was immobilized by gluing with Aron Alpha (Konishi Co., Ltd., Osaka, Japan) and one end of the electrode was soldered into two IC sockets with the soldered portion protected by surgical tape. For the other end of the electrode, we ensured that the front ends of two wires were split for 2 mm and the polyimide insulation on part of the wires (approximately 3 mm to the end) was peeled off for implantation.

Implantation of the electrode

During surgery, the animal was anesthetized with isoflurane (2%) mixed with air and placed in a stereotaxic frame to implant the stimulator electrode. The temperature of the animal was maintained at 37°C (monitored by a rectal thermostat probe) using a heating pad (Natsume Seisakusho Co., Tokyo, Japan). The scalp was removed to expose the cranium, and a small hole was drilled through the skull at the position above the left primary motor cortex (M1) (2.0 mm mediolateral, 2.0 mm anteroposterior from the bregma).^{10,11} Then the electrode was inserted into M1 (2.0 mm dorsoventral) according to the

stereotaxic co-ordinates¹² and immobilized by tissue Aron Alpha A adhesive (Sankyo Co., Ltd., Tokyo, Japan) covered with the dental cement GC UNIFAST II (GC Corporation, Tokyo, Japan).¹³ Figure 1a schematizes the position for electrode implanting above M1 of the rat brain in the right hemisphere.

MRI data collection

After surgery, the anaesthesia was changed from isoflurane to 0.1 mg/kg/h medetomidine (Orion Corporation, Espoo, Finland) with an initial bolus of 0.05 mg/kg. We inserted a catheter subcutaneously to ensure the continuous infusion of medetomidine via syringe pump (Harvard Apparatus, Holliston, MA, USA). Then the rats were mounted on the MRI bed fixed with ear bars and the rat's body temperature was maintained at 37°C throughout the experiments (CIRCU-LATING THERMO, Bruker Optik, Ettlingen, Germany). Body temperature was monitored by an ECG/TEMP module (SA Instruments Inc., NY, USA) and respiration was measured by a respiration module (SA Instruments Inc., NY, USA).

MR images were acquired using a 7T MRI system (Bio-Spec 70/20 USR, Bruker Optik, Ettlingen, Germany) and a surface coil was used for reception. BOLD fMRI data were acquired using a gradient echo-planar images (EPI) sequence with the following parameters: repetition time (TR) = 2 s, TE = 6.72 ms, flip angle = 30° , field of view = 24 mm \times 24 mm, acquisition matrix = 60 \times 60, voxel size = 0.4 mm \times 0.4 mm \times 1.6 mm, slice thickness = 1.5 mm, slice distance = 1.6 mm, slice number = 10. Structural images used for registration were obtained by a T_2 -weighted fast spin echo sequence with the following parameters: TR = 2500 ms, TE = 33 ms, field of view = 24 mm \times 24 mm, acquisition matrix = 256 \times 256, slice thickness = 1.5 mm, slice number = 10. The stimulation of M1 was devised as a block design with interleaved trials of stimulation off (60 s) and stimulation on (20 s) for a total duration of 5 min (three sessions). The electrical current was a pulse wave with frequency of 20 Hz and pulse width of 300 μs . The current intensity (0.3–0.6 mA) was chosen based on previous work,¹⁴ which selected 120% of the threshold for visible front limb movement. MRI data acquisition was synchronized with this stimulation protocol with a total of 150 volume images obtained. Figure 1b illustrates the time schedule of the experiment.

Data analysis

Analysis of the fMRI data was performed individually for each animal using MATLAB (MathWorks, Natick, MA, USA) and SPM12 (Wellcome Trust Centre for Neuroimaging, London, UK). Prior to statistical analysis, a series of pre-processing procedures were performed including a slice timing correction and realignment to correct residual head motion. The averaged fMR images were then co-registered to the anatomical images of each rat and all the fMR images were spatially normalized to a reference template (Tohoku University, Japan).¹⁵ We applied a Gaussian spatial smoothing filter with a full width at half maximum (FWHM) kernel of

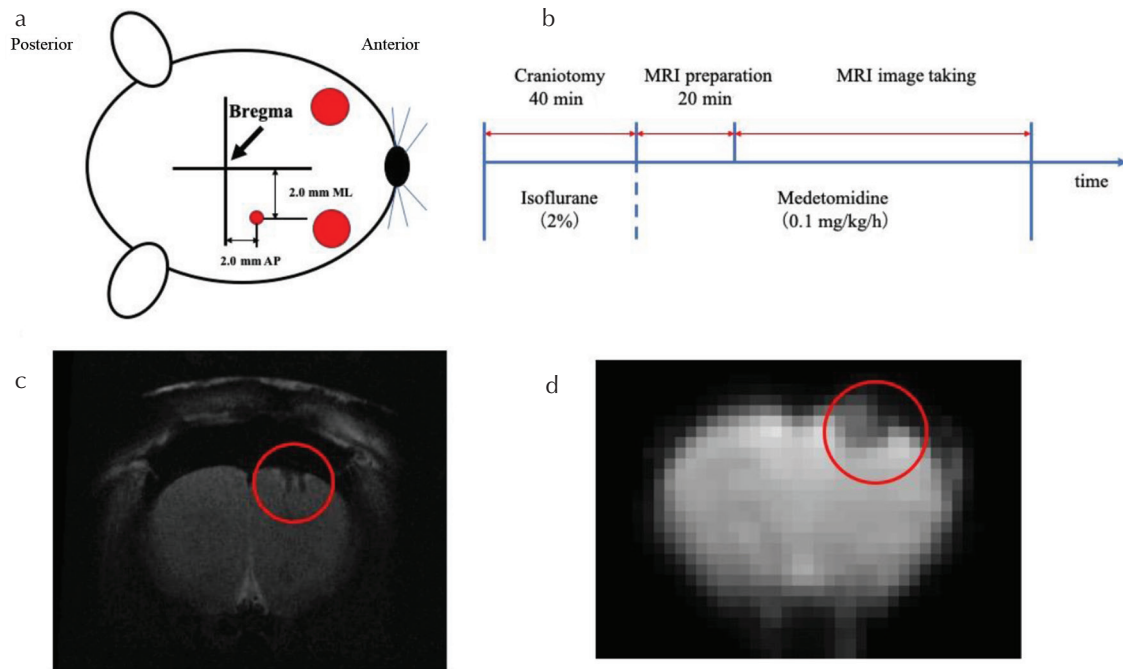


Fig. 1 Experimental design and confirmation of the electrode. (a) Precise coordinates for implanting the electrode referred to stereotaxic coordinates. (b) Time schedule for the experimental procedure. The anaesthesia was changed from isoflurane to 0.1 mg/kg/h medetomidine during the fMRI experiment. (c) Representative T_2 -weighted structural image of the rat model. The electrode could be discriminated from cortical tissue and lay in only one slice of the entire volume. (d) Representative echo-planar imaging of the same rat model. The electrode induced susceptibility artefacts in a relatively small region in the ipsilateral primary motor cortex (M1) in one slice.

0.6 mm (1.5 times the voxel size) to the normalized brain volumes to increase the signal-to-noise ratio (SNR) and improve the activation detectability. To address the concerns of the introduction of undesirable effects during the smoothing process, we also analysed our data without and with a smoothing FWHM kernel of 1 mm.

A general linear model-based statistical parametric analysis was individually used to depict the activation maps with a significance of $P < 0.001$ (uncorrected). The group analysis was performed using paired t -tests on the statistical results of each individual rat ($P < 0.05$, corrected cluster-level familywise error (FWE); equal to $P < 0.005$ uncorrected and minimum cluster size of 20 contiguous voxels). Region of interests (ROIs) were defined by referring to clusters deemed significant based on the group level analysis to further investigate the signal intensity changes in specific cortical structures activated by MCS via SPM toolbox MarsBaR (MRC Cognition and Brain Sciences Unit, Cambridge, UK) and MRIcron software (<http://www.cabiatl.com/mricron/mricron/install.html>). The number of significant activated voxels in each ROI were calculated across all the animals respectively according to their individual analysis results in MATLAB.

BOLD signal time series were individually calculated with respect to the baseline averaged over all the stimulation off period and the BOLD peak intensities, defined as the maximum signal change with respect to baseline, were identified and averaged over the three stimulation periods. Fitting curves were acquired by a moving average method with

period of three points. The time-to-peak was defined as the time to reach the maximum positive BOLD signal and the time to baseline was the time the BOLD signal returned to the baseline, both measured from the onset of stimulation.¹⁶

Statistical analysis

The statistical analysis was performed in MATLAB and Excel using t -tests and Tukey's multiple comparison test. A P -value of 0.05 was considered the threshold for significance. The results were reported as mean \pm standard error of the mean (SEM).

Results

We initially inspected the T_2 -weighted structural images across the entire rat brain to affirm the location of the electrode (Fig. 1c). We could easily discriminate our electrode from cortical tissue, and it lay in only one slice of the total volume. Additionally, in EPI we found that our tungsten electrode induced susceptibility artefacts exclusively in a small region in the ipsilateral primary motor cortex (M1) in one slice; however, these artefacts could potentially interfere with image acquisition (Fig. 1d). During the experiment, we observed a minor increase in the respiration rate of four animals, despite the lack of either strenuous movements or signs of waking up.

The activation maps for each animal were made individually and Fig. 2a demonstrates a representative result of the

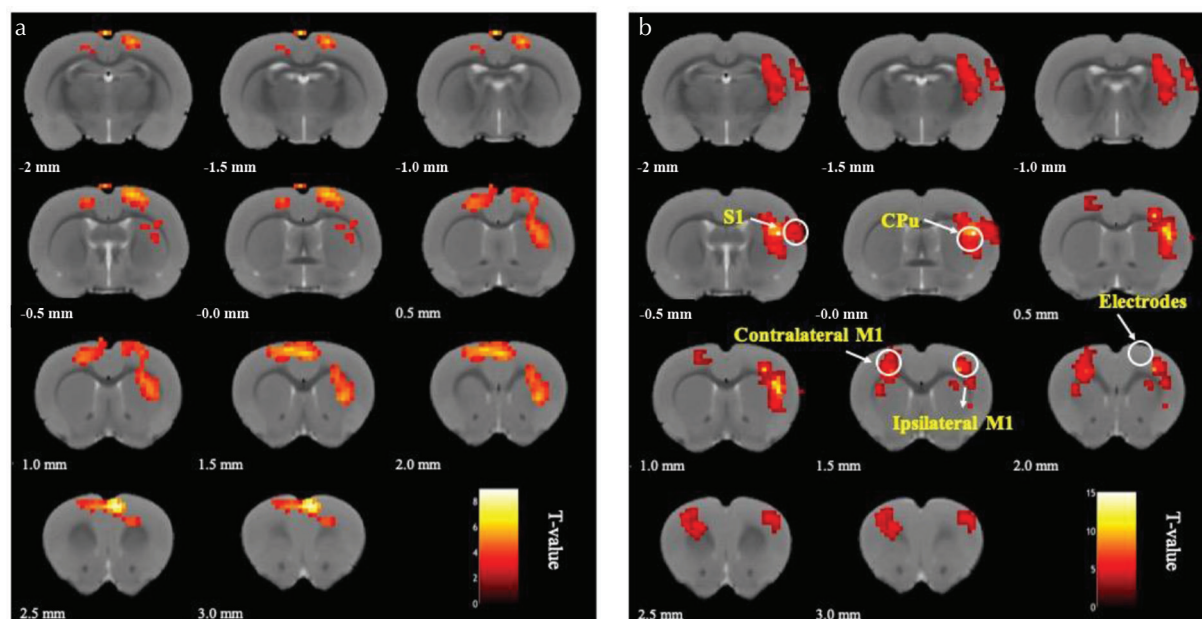


Fig. 2 Activation maps depicted by SPM12 based on a general linear model. (a) A representative activation map of the same animal from Fig. 1c ($P < 0.001$, uncorrected). (b) The activation map of group analysis results ($n = 8$, cluster-level FWE of $P = 0.05$). Obvious blood oxygen-level dependent signal changes mainly distributed at M1 on the contralateral side of the stimulation spot and the primary somatosensory cortex (S1), as well as the caudate-putamen (CPu) on the ipsilateral side. Due to the interference of the inserted electrode, the signal in the ipsilateral M1 was scattered around the insertion area.

same animal from Fig. 1c. Next, an activation map of the group analysis (Fig. 2b) was depicted across all the animals ($n = 8$) with a threshold of $P < 0.005$ (uncorrected, minimum cluster size of 20 contiguous voxels) set to restrict a cluster-level FWE of $P = 0.05$. MCS-evoked BOLD signal changes in focal regions in the slices positioned from 2.0 mm posterior to 3.0 mm anterior to the bregma. These evident BOLD signal changes were mainly distributed at M1 on the contralateral side of the stimulation spot, the primary somatosensory cortex (S1), and caudate-putamen (CPu) on the ipsilateral side. Due to interference of the inserted electrode, we failed to observe any significantly activated signal at the insertion position, only scattered around the insertion area (still part of M1). The distribution of the activation signals were quite localized and no negative BOLD signals were found.

To further investigate the BOLD signal time courses in these regions, we chose a ROI according to clusters of statistical results by SPM respectively and analysed signal intensity changes along with the scan time (volume number). The final time course graphs were made by averaging the subjects that demonstrated activation regions corresponding to the single subject analysis (Fig. 3). By correlating the stimulus period with the BOLD time course, we found that the BOLD signals occurred in conjunction with the onset of the electrical stimulation. There were no BOLD responses found in the CPu or S1 on the contralateral side of the stimulation spot (Fig. 3e and 3f). The number of significant activated voxels in the ipsilateral M1, contralateral M1, CPu, and S1 were 27 ± 51 , 283 ± 106 , 330 ± 56 , 224 ± 67 , respectively.

Next, the average times for the BOLD signal to reach its peak and to decline back to baseline and the maximum signal magnitude of each stimulation session are shown in Fig. 4. The results demonstrated that the BOLD signal variation in all four regions shared similar temporal characteristics in that the BOLD signal waves in distinct regions rose to the peak at approximately the same time point (multiple-comparison Tukey test with significant level of $P = 0.05$), which was simultaneous to the stimulation period (Fig. 4a and 4b). Once the stimuli were halted, the BOLD signal displayed a downward trend and gradually recovered to baseline after approximately 20 volumes (40 s) post-stimuli onset (Fig. 4d).

As for the maximum signal intensity, we found that the first session of stimulation generated similar magnitudes of BOLD response in all regions, but the intensity of the second BOLD signal was attenuated. In the CPu particularly, we observed that during the second session of stimulation, this region demonstrated a minimal response against it, while in the third session, the BOLD signal change recurred. Furthermore, we have enough evidence to be suspicious of the peak intensity in the ipsilateral M1. We have described above that the implanted electrodes interfered the signal collection in this area, which might consequently cause the degradation of the signal magnitude.

Discussion

Although many studies have focused on MCS, most have emphasized the neural response in the post-therapy stage;^{4,7}

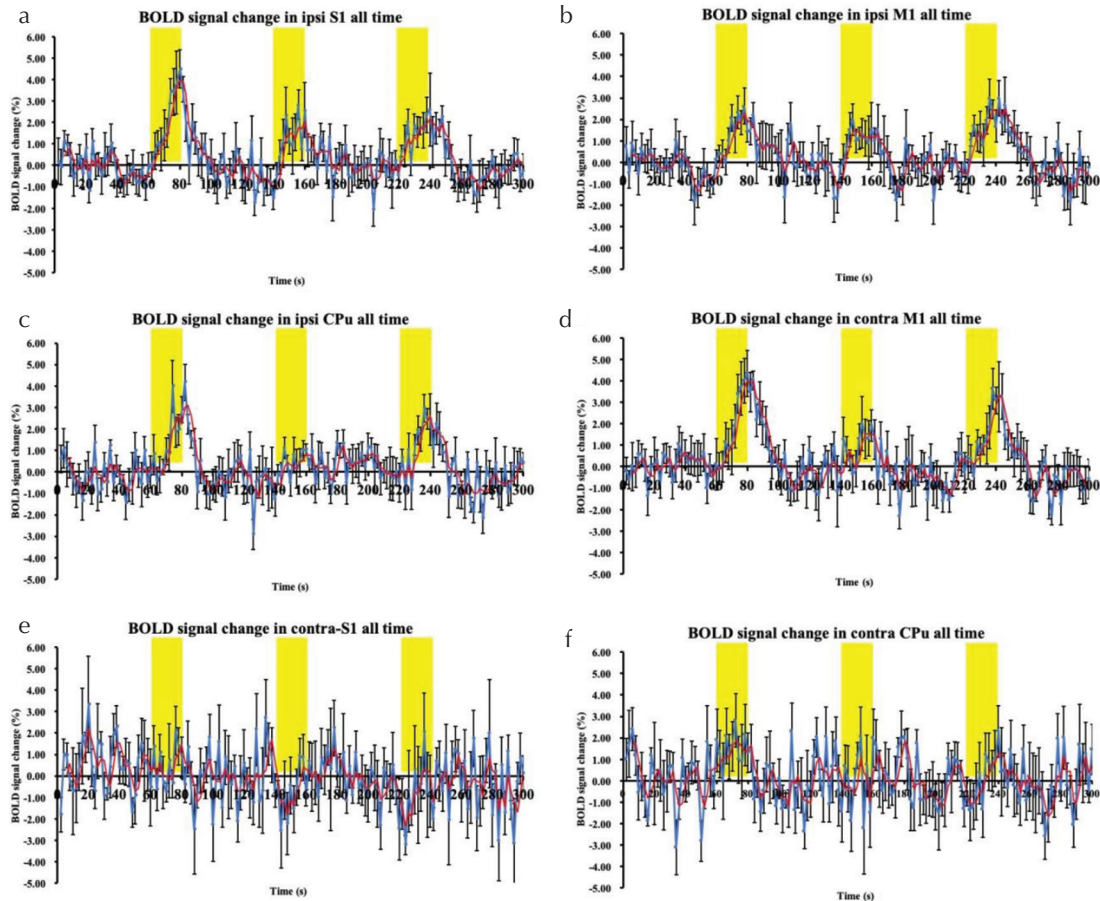


Fig. 3 Blood oxygen-level dependent (BOLD) signal time course for all time in primary motor cortex (M1), primary somatosensory cortex (S1), and caudate-putamen (CPu). (a) Ipsilateral S1. (b) Ipsilateral M1. (c) Ipsilateral CPu. (d) Contralateral M1. (e) Contralateral S1. (f) Contralateral CPu. The yellow boxes represent electrical stimulation periods. The bar plots exhibit mean \pm standard error of the mean (SEM). Fitting curves in red were acquired by a moving average method with period of three points.

however, the investigation of the brain activation during the MCS procedure is essential. Tungsten is an appropriate material because it reduces the magnetic susceptibility artefacts better than commercially available MR-compatible platinum-iridium electrodes.

In the present study, we implemented fMRI experiments simultaneously with intracortical MCS in rat models to investigate potential neural pathways during MCS. We obtained positive BOLD responses in the bilateral M1, ipsilateral S1, and ipsilateral striatum. Moreover, no negative signals were found in our results. According to the BOLD signal time course of these three encephalic regions, we also found that the signal intensity changes reached a peak at the same time point, indicating that the neural activation of these regions occurred synchronously.

For these activated neural regions, many studies have reported that all of them are closely associated with nociceptive or analgesic procedures. In a few studies on surgically anesthetized animals, It has been demonstrated that the relationships within nociceptive stimulation and the activation of neurons are similar at the subcortical levels of

somatosensory projection and within the primary S1.¹⁷ Another report using preclinical and clinical data of human, determined that the basal ganglia is uniquely involved in the cortico-striato-thalamo-cortical loop to integrate several aspects of pain suggested by alterations in cortical and subcortical regions in pain.¹⁸ For M1, current evidence based on the research of Phantom Limb Pain has suggested a relationship between chronic pain and motor-cortex reorganization. Additionally, evidence has accumulated describing that interventions in normalizing motor-cortex organization can lead to pain relief.¹⁹

Our results also demonstrate a widely argued notion that mechanisms of MCS involve the activation of areas that are distant from the site of the stimulation. Previous studies have authenticated a mechanism that stimulation in M1 evoked localized activity changes in subcortical structures.^{19,20} One study, which measured BOLD MRI signal changes during high frequency rTMS in humans, reported obvious signal changes in the ipsilateral putamen²⁰ and our results with the rat model are consistent with this phenomenon. Since a portion of the putamen is thought to receive sensorimotor

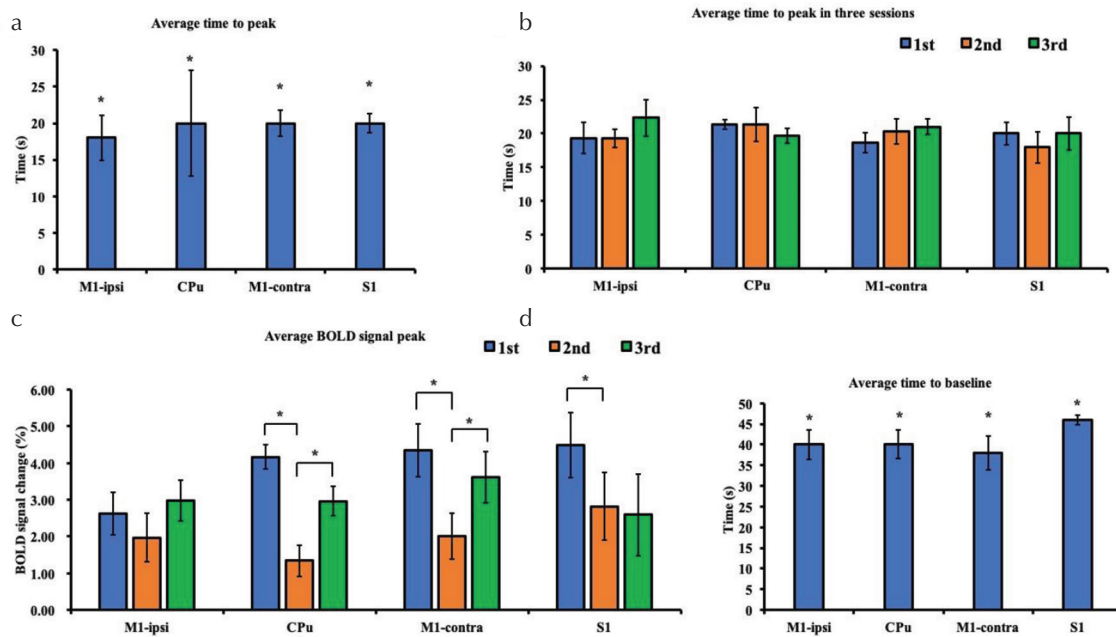


Fig. 4 BOLD response parameters in the bilateral M1, ipsilateral CPu, and ipsilateral S1. **(a)** Average time to peak. $^*P < 0.05$ (multiple comparison Tukey's test across four regions, the average time to peak showed no significant difference). **(b)** Average time to peak in three sessions. **(c)** Average BOLD signal intensity peak in three stimulation sessions individually. $^*P < 0.05$ (multiple comparison Tukey's test across three stimulation sessions in each region, the mean BOLD intensity change in the second intensity change is different from the first and third). **(d)** Average time to baseline. $^*P < 0.05$ (multiple comparison Tukey's test across four regions, the average recover time showed no significant difference). The bar plots exhibit mean \pm SEM. BOLD response to the second stimulation session collapsed and recovered during the third.

projections,²¹ this may offer a possible explanation of our results. Nevertheless, authors of this study also reported activation in the ipsilateral ventrolateral thalamus, which is known to be intimately associated with the sensorimotor cortex. We did not observe changes in this region in our rat model, which might be the result of the use of anaesthesia for animal sedation, as well as the restrictions of the stimulation scope; these are both limitations that are worth investigating in future work. Additionally, in our work a relatively short TE and a small flip angle were selected for improving the SNR, this may also account for the absence of signal.

Austin et al.¹⁴ demonstrated that BOLD fMRI signal changes against unilateral M1 stimulation could be yielded in both the stimulated and homotypic contralateral cortices, which is in accordance with a portion of the subjects ($n = 5$) in our results. However, due to the interference of the implanted electrodes, BOLD signal responses of the cortex that lie in the stimulation position were not observed in the rest of the subjects or in the group analysis results. For the BOLD signal changes that arose at the contralateral cortex regions, we found that the spatial distribution was relatively concentrated and had no sign of spread. This may demonstrate that activation of the contralateral cortex is unlikely to occur through the spread of the electrical stimulation, but due to the functional connectivities of the rodent M1. We also found that in our BOLD signal time course analysis, the temporal characteristics of M1 ipsilateral to the stimulation spot

($n = 5$) and M1 in the contralateral position produced similar patterns. This phenomenon can be explained by a mechanism that allows simultaneous information processing to continue by neurons located in different regions of the cortex. In Austin et al.'s study,¹⁴ they described the occurrence of changes in the BOLD signal in the ipsilateral striatum, in only two subjects, while our results strongly suggested that this encephalic activation can be reproduced across individuals. Another observation of the BOLD time course in our results is that the first session of stimulation generated similar magnitudes of BOLD response in all regions, but the response to the second stimulation session collapsed and recovered during the third (Fig. 4c). This phenomenon is similar, as it was observed by Riemann et al.,²² therefore can be explained by heavy neuronal after-discharges caused by the first stimulation session.

Notwithstanding the principal target of M1, the results of the present study are similar to portions of work done by Cho et al.,²³ who conducted direct electrical nerve stimulation of the rat upper extremity. They recapitulated that the antidromic stimulation of motor nerve fibres is a possible explanation for why these regions can be activated or inhibited after they receive nociceptive impulses. Alternatively, opto-fMRI is another methodology to intrinsically investigate MCS response. Lee et al.²⁴ observed activity in the thalamus after light stimulation of ChR2-expressing neurons in M1 using a rat model expressing ChR2 in the excitatory neurons

of the motor cortex. Since the CPu is involved in both the somatosensory and motor neural networks of the rat, which have direct connections to the motor cortex, the thalamic nuclei, or both, we postulate whether thalamic regions could be a plausible extension of our results.

In this study, we focused on the encephalic regions that provide an instant response to the motor cortical stimulation process in healthy rat models. Whether our conclusion can be universally accepted in both healthy and neuropathic pain models remains a valid concern, considering the fact that numerous studies have reported that chronic pain in rodent model may considerably change brain function and connectivity.^{25,26} However, this claim needs to be further investigated. Nevertheless, it is our understanding that our results may help elucidate the neural signal propagation after the onset of MCS and establish a direct cortical stimulation rodent model in combination with fMRI; furthermore, this model is extensible even in animals presenting with neuropathic pain.

Conclusion

We conducted an fMRI experiment simultaneously with direct electrical stimulation to the unilateral motor cortex of rats via a custom-made tungsten bipolar electrode to investigate the functional connectivity and the function mapping during MCS. The bilateral M1, ipsilateral primary S1, and ipsilateral CPu were observed to be activated during MCS and the signal time courses in these areas were analysed. To the best of our knowledge, only a few studies have been conducted on direct cortical stimulation of the rodent brain to investigate its instant effect using fMRI; reproducible results in the CPu have not been previously found. We anticipate our results to be effective to the establishment of neural pathways involved in MCS.

Acknowledgments

This work was supported by a Grant-in-Aid for Research Fellowships of the Japan Society for the Promotion of Science (JSPS Research Fellow) under grant number 18J00922 (Y.A.). We gratefully acknowledge the help from J. Gu and D. Kim for supporting the experiment and animal handling.

Author Contributions

Z.X., K.F.T., K.H., Y.S. and M.S. designed research, Z.X., Y.A. and S.L. performed research, Z.X. analyzed data, Z.X., Y.A., M.S. discussed the interpretation of the results, and Z.X. wrote the paper. All authors revised the final manuscript.

Conflicts of Interests

The authors declare no competing interests.

References

1. Costigan M, Scholz J, Woolf CJ. Neuropathic pain: a maladaptive response of the nervous system to damage. *Annu Rev Neurosci* 2009; 32:1–32.
2. Peyron R, Faillenot I, Mertens P, Laurent B, Garcia-Larrea L. Motor cortex stimulation in neuropathic pain. Correlations between analgesic effect and hemodynamic changes in the brain. A PET study. *Neuroimage* 2007; 34:310–321.
3. Lefaucheur J, Drouot X, Ménard-Lefaucheur I, Keravel Y, Nguyen JP. Motor cortex rTMS restores defective intracortical inhibition in chronic neuropathic pain. *Neurology* 2006; 67:1568–1574.
4. Delavallée M, Abu-Serieh B, de Tourchaninoff M, Raftopoulos C. Subdural motor cortex stimulation for central and peripheral neuropathic pain: a long-term follow-up study in a series of eight patients. *Neurosurgery* 2008; 63:101–105; discussion 105–108.
5. Lefaucheur JP, Ménard-Lefaucheur I, Goujon C, Keravel Y, Nguyen JP. Predictive value of rTMS in the identification of responders to epidural motor cortex stimulation therapy for pain. *J Pain* 2011; 12:1102–1111.
6. Garcia-Larrea L, Peyron R. Motor cortex stimulation for neuropathic pain: from phenomenology to mechanisms. *Neuroimage* 2007; 37:S71–S79.
7. Lucas JM, Ji Y, Masri R. Motor cortex stimulation reduces hyperalgesia in an animal model of central pain. *Pain* 2011; 152:1398–1407.
8. Jiang L, Ji Y, Voulalas PJ, et al. Motor cortex stimulation suppresses cortical responses to noxious hindpaw stimulation after spinal cord lesion in rats. *Brain Stimul* 2014; 7: 182–189.
9. Lai HY, Albaugh DL, Kao YC, Younce JR, Shih YY. Robust deep brain stimulation functional MRI procedures in rats and mice using an MR-compatible tungsten microwire electrode. *Magn Reson Med* 2015; 73:1246–1251.
10. Kim D, Chin Y, Reuveny A, Sekitani T, Someya T, Sekino M. An MRI-compatible, ultra-thin, flexible stimulator array for functional neuroimaging by direct stimulation of the rat brain. *Conf Proc IEEE Eng Med Biol Soc* 2014; 2014: 6702–6705.
11. Fonoff ET, Pereira JF, Camargo LV, et al. Functional mapping of the motor cortex of the rat using transdural electrical stimulation. *Behav Brain Res* 2009; 202:138–141.
12. Paxinos G, Watson C. The rat brain in stereotaxic coordinates: hard cover edition, Cambridge, Massachusetts, United States, Elsevier, 2006.
13. Abe Y, Sekino M, Terazono Y, et al. Opto-fMRI analysis for exploring the neuronal connectivity of the hippocampal formation in rats. *Neurosci Res* 2012; 74:248–255.
14. Austin VC, Blamire AM, Grieve SM, et al. Differences in the BOLD fMRI response to direct and indirect cortical stimulation in the rat. *Magn Reson Med* 2003; 49:838–847.
15. Valdés-Hernández PA, Sumiyoshi A, Nonaka H, et al. An in vivo MRI template set for morphometry, tissue segmentation, and fMRI localization in rats. *Front Neuroinform* 2011; 5:26.
16. Abe Y, Tsurugizawa T, Le Bihan D, Ciobanu L. Spatial contribution of hippocampal BOLD activation in high-resolution fMRI. *Sci Rep* 2019; 9:3152.

17. Vierck CJ, Whitsel BL, Favorov OV, Brown AW, Tommerdahl M. Role of primary somatosensory cortex in the coding of pain. *Pain* 2013; 154:334–344.
18. Borsook D, Upadhyay J, Chudler EH, Becerra L. A key role of the basal ganglia in pain and analgesia - insights gained through human functional imaging. *Mol Pain* 2010; 6:27.
19. Mercier C, Léonard G. Interactions between pain and the motor cortex: insights from research on phantom limb pain and complex regional pain syndrome. *Physiother Can* 2011; 63:305–314.
20. Bestmann S, Baudewig J, Siebner HR, Rothwell JC, Frahm J. Functional MRI of the immediate impact of transcranial magnetic stimulation on cortical and subcortical motor circuits. *Eur J Neurosci* 2004; 19:1950–1962.
21. Parent A, Hazrati LN. Functional anatomy of the basal ganglia. I. The cortico-basal ganglia-thalamo-cortical loop. *Brain Res Brain Res Rev* 1995; 20:91–127.
22. Riemann S, Helbing C, Angenstein F. From unspecific to adjusted, how the BOLD response in the rat hippocampus develops during consecutive stimulations. *J Cereb Blood Flow Metab* 2017; 37:590–604.
23. Cho YR, Pawela CP, Li R, et al. Refining the sensory and motor ratunculus of the rat upper extremity using fMRI and direct nerve stimulation. *Magn Reson Med* 2007; 58:901–909.
24. Lee JH, Durand R, Gradinaru V, et al. Global and local fMRI signals driven by neurons defined optogenetically by type and wiring. *Nature* 2010; 465:788–792.
25. Chao TH, Chen JH, Yen CT. Plasticity changes in forebrain activity and functional connectivity during neuropathic pain development in rats with sciatic spared nerve injury. *Mol Brain* 2018; 11:55.
26. Da Silva JT, Seminowicz DA. Neuroimaging of pain in animal models: a review of recent literature. *Pain Rep* 2019; 4:e732.